J. Phys.: Condens. Matter **20** (2008) 304211 (7pp) doi:10.1088/0953-8984/20/30/304211

Anderson localization regime in carbon nanotubes: size dependent properties

F Flores[1], B Biel[1,5], A Rubio[2,3], F J Garcia-Vidal[1], C Gomez-Navarro[4], P de Pablo[4] and J Gomez-Herrero[4]

[1] Departamento de Fisica Teórica Materia Condensada, Universidad Autónoma de Madrid, 28049-Madrid, Spain
[2] European Theoretical Spectroscopy Facility (ETSF), Departamento de Fisica de Materiales, Universidad Pais Vasco, Edificio Korta, Avd. Tolosa 72, 20018 San Sebastian, Spain
[3] Unidad de Física de Materiales Centro Mixto CSIC-UPV/EHU and Donostia International Physics Center (DIPC), 20018 San Sebastian, Spain
[4] Departamento de Física Materia Condensada, Universidad Autónoma de Madrid, 28049-Madrid, Spain

Received 14 December 2007, in final form 12 February 2008
Published 8 July 2008
Online at stacks.iop.org/JPhysCM/20/304211

Abstract
The influence of disorder and defects is of fundamental relevance in the performance of nanotube-based devices. It is then crucial to understand the properties of (as-grown or *in situ* created) defects in order to conquer their detrimental effects, but also to tune nanotube properties in a desired direction. We show experimentally and theoretically the formation, in different single-walled carbon nanotubes, of a strong Anderson localization regime in which the electrical resistance increases exponentially with the length of the nanotube. This implies that, in these systems, the coherence length can be much longer than the localization length. We also show how the localization length depends strongly on the tube diameter and it increases as the tube diameter is enlarged. Furthermore, we analyse in detail the role of temperature on electron localization, demonstrating that this strong localization regime survives to nearly room temperature: the net effect of the temperature is to wash out the strong fluctuations that appear at zero temperature.

(Some figures in this article are in colour only in the electronic version)

1. Introduction

Although one-dimensional (1D) disordered systems have been carefully analysed [1] and their density of states, conductance probability distribution, average resistance, nature of wavefunctions dominating the transmission process and characteristic noise, have also been calculated using different approximations [2, 3], there is still a lack of understanding of how temperature affects, in these systems, the resistance and its fluctuations as a function of the length of the system. On the other hand, in spite of the great development achieved in the last 10 years in the field of nano-science and in the preparation of 1D systems, up to the best of our knowledge, there is no clear realization of 1D disordered structures, where a careful analysis of the theory's predictions could be carried out.

[5] Present address: CEA, LETI-MINATEC, 17 rue des Martyrs, 38054 Grenoble, Cedex 9, France.

Carbon nanotubes [4] are a good realization of nearly 1D systems where both basic science and potential nanodevice applications merge. The electronic properties of nanotubes are strongly modulated by small structural variations. In particular, their metallic or semiconducting character is determined by the diameter and helicity (chirality) of the carbon atoms forming the nanotube. A recent review of electronic and transport properties of carbon nanotubes can be found in [5] and ones on the fundamentals and applications of nanotubes in the books by Loiseau *et al* [6], Ebbesen [7], Christopher [8] and Dresselhaus *et al* [9] (and references therein).

On the other hand, carbon nanotubes offer an excellent possibility for analysing their transport properties as a function of their randomly distributed defects. The influence of defects is of fundamental relevance in the performance of electronic and transport properties of carbon materials, in particular for molecular sensor devices. Substitutional doping by N or B impurities on carbon nanotubes has been a very intense

research topic at the experimental and theoretical level during recent years. Initial works have focused on the effect of a single defect on the electronic and transport properties, while further studies have addressed the issue of mesoscopic transport in nanotubes with random distributions of impurities. The influence of defects is also of fundamental importance in the performance of electronic and sensing devices based on carbon nanostructures. Switching from ballistic to either the weak or strong localization transport regime is possible above a certain density of defects. Defect sites augment the chemical reactivity of nanotube walls, rendering them sensitive to certain chemical species, as well as to tailor their properties for specific nanodevice applications.

The main problem when analysing the effects of disorder on the transport properties is controlling carefully the number of defects in the nanotube. This problem has been nicely overcome in [10] by *in situ* irradiation of single-walled carbon nanotubes (SWNTs) with Ar^+: these ions mainly create di-vacancies in the nanotube [11] and a systematic control of the irradiation dose allows an appropriate determination of the density of nanotube di-vacancies, which can be expected to be randomly distributed along the structure.

In this paper we follow our previous works and analyse in detail how argon irradiation modifies the transport properties of different SWNTs: in particular, here we present detailed results for (5, 5) nanotubes and compare them with the (10, 10) case, previously reported in [10, 12]. This analysis will allow us to obtain how the localization regime depends on the diameter of the SWNTs and, last but not least, how temperature modifies their transport properties, localization length and average resistance as a function of the nanotube diameter.

2. Electronic transport regimes in carbon nanotubes. The Anderson localization regime

Before analysing the strong Anderson localization regime in SWNTs, it is worth discussing qualitatively the different electron transport regimes [13] that are expected to be observed in these systems. Figure 1 shows schematically the regimes which have been already observed. For completeness, we should also mention the Luttinger-liquid regime, although, to the best of our knowledge, it is not clear whether this regime has been settled beyond reasonable doubt.

Figure 1 illustrates for one-dimensional systems how the three different regimes, (a) ballistic, (b) diffusive and (c) localized, are determined.

(a) In the ballistic regime, electrons propagate between the two electrodes without suffering either elastic or inelastic processes inside the nanotube. The condition for this regime to appear is for the nanotube length, L, to be smaller than either L_0, the localization length associated with the impurities of the system, or L_φ, the coherence length associated with the inelastic processes the electrons may suffer ($L < L_0, L_\varphi$). In this case, there is no voltage drop along the nanotube, but there appears a voltage drop in the contacts yielding a total resistance of $R_0/2$ ($R_0 = 1/G_0$, G_0 being the conductance quantum), where the factor $1/2$ is due to the two channels of the nanotube. As shown in figure 1(a), the chemical potential is constant along the nanotube and the contact voltage drop is associated with the jump in the chemical potentials between the nanotube and the reservoirs.

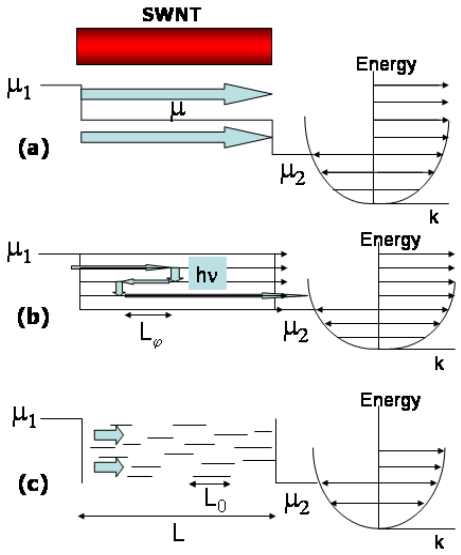

Figure 1. Different regimes are determined by L (nanotube length), L_0 (localization length) and L_φ (coherence length).

(b) In the diffusive regime (see figure 1(b)), the inelastic electron–phonon interaction is dominant and, in this case, L_φ is smaller than both L and L_0 ($L_\varphi < L, L_0$). In this regime electrons are scattered off by phonons, and the transport process is controlled by the diffusive propagation of electrons. In this limit, one can expect to have a kind of Ohm's law; although this regime has been observed at very low bias and very clean samples (then, L_0 is very long), changes with respect to this law have been found for high enough bias (higher than the energy of the optical phonons in the nanotube) [14].
We should comment at this point that the Luttinger-liquid regime can be expected to dominate the nanotube transport process if the corresponding incoherent length, say L'_φ, is shorter than the other lengths of the problem, say L, L_0 and L_φ. It is not clear, however, if this limit can be reached in the SWNTs.

(c) In the limit of a large number of impurities and low bias voltage the strong Anderson localization regime dominates the transport process [12, 15] (see figure 1(c)). In this limit, electrons become localized by the random potential of the defects. Typically (see below), the localized electron wavefunctions have a size of the order of L_0. Therefore, electrons can only propagate from one electrode to the other by a tunnelling process that yields an exponential dependence of the nanotube resistance versus the length of the nanotube, $R \sim R_0 \exp(L/L_0)$.

In this paper we are interested in analysing the last regime, the strong Anderson localization regime, a limit for which $L_0 < L < L_\varphi$. If the coherence length is longer than L, we can neglect the inelastic processes for the electrons. Additionally,

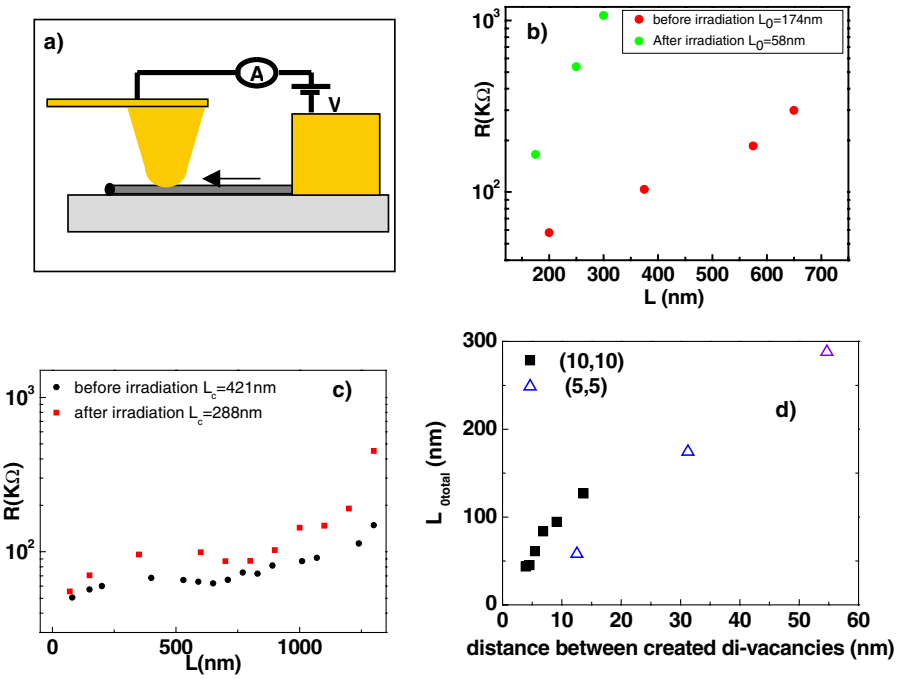

Figure 2. (a) Scheme of the experimental set-up used to measure the SWNT conductance, showing a gold covered tip, the SWCNT and the gold electrode. (b) SWNT resistance versus length for a (5, 5) SWNT before and after Ar^+ irradiation. (c) As panel (b) but for a smaller Ar^+ irradiation. (d) Localization length as a function of the distance between di-vacancies for (5, 5) and (10, 10) SWNTs.

if the nanotubes have enough impurities to satisfy the condition $L_0 < L$, the system enters into the localization regime. These two conditions imply (i) probing nanotubes' lengths about or smaller than 1 μm, the order of magnitude of the mean free path associated with the electron–phonon interaction [14], and (ii) the mean distance between di-vacancies must be around or smaller than 100–200 nm (this condition comes from the rule discussed in section 5 that L_0 is around 5–10 times the distance between di-vacancies, the impurities created in the nanotube with Ar^+ irradiation, see section 3).

3. Experiments

The experiments are performed using conductance force microscopy [16]. Briefly, with this technique a metallized AFM tip is used as a mobile electrode. Samples consist of a random distribution of SWNTs deposited on an insulating substrate where a macroscopic gold electrode has been evaporated. SWNTs contacted to the electrode are found using the non-contact dynamic mode. Once a particular nanotube is selected, the tip is brought into contact with the nanotube and a voltage is applied. Finally, the electrical current flowing through the nanotube is acquired (see figure 2(a)). By repeating this procedure at different pre-selected spots along the tube, it is possible to obtain resistance versus length curves, $R(L)$ [17]. For this study, the selected SWNTs present diameters of 1.4 ± 0.2 nm and 0.6 ± 0.2 nm, which are compatible with (10, 10) and (5, 5) chiralities, respectively.

All the commercial SWNTs analysed in our experimental study [10] show an exponential dependence of resistance on the length of the tube, attributed to the Anderson localization regime, due to the presence of defects in the tubes caused by the SWNT preparation technique. For 'clean' metallic nanotubes directly grown on a surface by chemical vapour deposition [14], $R(L)$ at low voltage presents a linear dependence with a resistivity of 10 ± 2 K Ω/microns. This number is in perfect agreement with those obtained with experiments in which many nanoelectrodes are placed along the SWNT length [18]. The experimental data for commercial samples can be fitted to $R(L) = R_c + R_0 \exp(L/L_0)$, where R_c is the contact resistance, R_0 is the quantum of resistance, and L_0 is the localization length. Localization lengths for non-irradiated nanotubes are in between 50 and 450 nm.

After a first electrical characterization as mentioned above, nanotubes are irradiated with a controlled dose of Ar^+ ions at 120 eV in order to create defects. Ar^+ irradiation at this energy is known to create both mono-and di-vacancies at a rate of 3–1 [11]. After each dose of irradiation, we electrically characterize again the same nanotube in order to track changes in their resistance, finding a decrease in the localization length (figure 2(b)). This is expected in the Anderson localization regime as the number of defects is increased after the SWNT being irradiated. Measuring the current, sample area, and nanotube diameter, we can estimate the number of di-vacancies created during the irradiation process and, eventually, plot the localization length as a function of the number of di-vacancies (the defects mainly responsible for the electron scattering, as we will show below) for both (10, 10) and (5, 5) nanotubes (figure 2(c)); this has been done by assuming that three Ar^+ ions create one di-vacancy, in agreement with [10, 11].

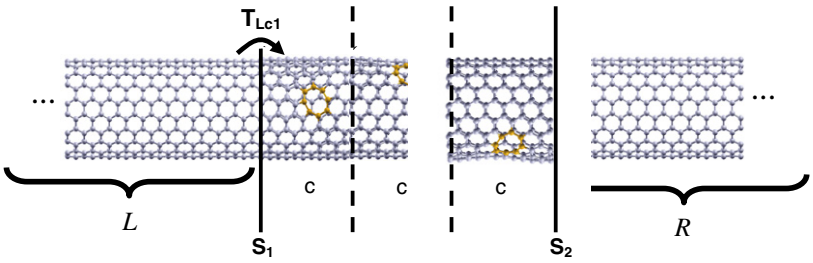

Figure 3. Schematic picture of the defected nanotube coupled to two electrodes (L and R).

4. Method of calculation and defects

In order to calculate the relaxation around the defects we have used a first-principles local orbital density functional method in which the electron density is expanded in terms of a sp^3-basis set of FIREBALL orbitals [19]. In this way, we can calculate the most stable geometries for the defects and their neighbouring atoms and, at the same time, feed the tight-binding Hamiltonian that is the basis of our Green's function technique to analyse the transport of electrons through the defected nanotube. In what follows we describe the main ingredients of this theoretical framework that, as we will demonstrate, is ideally suited to treat electron transport properties of carbon nanotubes in which a large number of defects (di-vacancies) are distributed along the tube.

In general, we are interested in the conductance, G, for a defected nanotube. The simulation geometry consists of a device region with the defected nanotube connected to two semi-infinite perfect tubes that act as left and right electrodes (see figure 3). In this approach, the differential conductance $g(E)$ is calculated at the tube–lead interface S_2 by means of the equation [20]

$$g(E) = \frac{4\pi e^2}{\hbar}\mathrm{Tr}\left[\hat{D}^A_{LL}(E)\hat{T}_{L2}\hat{\rho}_{22}(E)\hat{T}_{2L}\hat{D}^R_{LL}(E)\hat{\rho}_{LL}(E)\right] \tag{1}$$

where Tr represents the trace of the operator in brackets. $\hat{T}_{L2}$ describes the coupling between the right end of the nanotube (which contains the semi-infinite lead 1 plus the defected nanotube) and lead 2, $\hat{\rho}_{22}(E)$ being the density of states matrix associated with the decoupled ($\hat{T}_{L2} = 0$) semi-infinite lead 2 projected at S_2 and related to the retarded Green's function ($\hat{g}^R_{22}$) by $\hat{\rho}_{22} = -1/\pi\,\mathrm{Im}\,\hat{g}^R_{22}$; for calculating $\hat{g}^R_{22}$ we use standard decimation techniques. $\hat{\rho}_{LL}(E)$ is the density of states matrix projected onto the right end of the nanotube and is calculated by an iterative procedure. Let us describe briefly this numerical procedure that has some strong similarities with the transfer matrix technique used by Professor Pendry on many occasions. The defected nanotube (c) is divided into several portions each containing a single defect, $c = c_1 + c_2 + c_3 + \cdots$. The iterative procedure starts with the *uncoupled* semi-infinite perfect lead 1, characterized by a retarded Green's function $\hat{g}^{R(0)}_{LL}$ (that, like the one corresponding to lead 2, can be calculated by decimation techniques). In the first step we append the first defected section c_1 to lead 1 by using Dyson equation. The retarded Green's function of section c_1, $\hat{g}^R_{c_1c_1}$, is written as a function of its corresponding Hamiltonian matrix, $\hat{H}_{c_1}$, and the projection of the left electrode, $\hat{\Sigma}_{\mathrm{L}}(E)$, onto it:

$$\hat{g}^R_{c_1c_1} = \left[E + \mathrm{i}\eta - \hat{H}_{c_1} - \hat{\Sigma}_{\mathrm{L}}(E)\right]^{-1} \tag{2}$$

where $\eta \to 0^+$ and the projection $\hat{\Sigma}_{\mathrm{L}}(E)$ depends on the Green's function of the *uncoupled* lead 1 and the coupling matrix between lead 1 and section c_1, $\hat{T}_{Lc_1}$ (see figure 3):

$$\hat{\Sigma}_{\mathrm{L}}(E) = \hat{T}_{c_1L}\hat{g}^{R(0)}_{LL}(E)\hat{T}_{Lc_1}. \tag{3}$$

In the second step, section c_2 is appended to section c_1 (that contains the projection of lead 1) using equations similar to equations (2) and (3). After N steps, we build the whole tube and their corresponding retarded and advanced Green's functions $\hat{g}^{R(A)}_{LL}$ that are needed to feed equation (1). The main advantage of this numerical procedure is that, at each step, we have to invert a matrix whose dimensions are controlled by the size of each defected region and not by the size of the whole defected nanotube. In this way, we can include straightforwardly a random configuration containing a huge number of defects distributed along the nanotube, with a given mean distance between them. The retarded and advanced denominator functions $\hat{D}$ appearing in equation (1) are given by

$$\hat{D}^{R(A)}_{LL}(E) = \left[I - \hat{g}^{R(A)}_{LL}(E)\hat{T}_{L2}\hat{g}^{R(A)}_{22}(E)\hat{T}_{2L}\right]^{-1} \tag{4}$$

At zero temperature, the low bias conductance G is calculated by just evaluating g at the Fermi energy, $g(E_{\mathrm{F}})$. If we are interested in obtaining G at a temperature T, we have to evaluate the following integral: $G = \int_{-\infty}^{\infty}(-\frac{\mathrm{d}f_T}{\mathrm{d}E})g(E)\mathrm{d}E$, where $f_T(E) = \frac{1}{\mathrm{e}^{\frac{E-E_{\mathrm{F}}}{k_{\mathrm{B}}T}}+1}$ is the Fermi distribution function and k_{B} the Boltzmann constant.

5. Nanotube resistance, localization length and temperature effects

One-dimensional systems enhance the wave-like nature of electrons, introducing important corrections in their transport properties, which depend on the quantum interferences associated with the boundary conditions and the existing material impurities. In these 1D systems, electron transmission through static scattering centres will depend critically on the energy of the incoming electron and the distance between

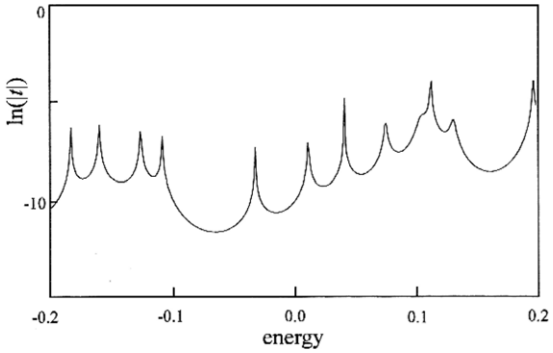

Figure 4. Transmission as a function of energy for a one-dimensional system. Reproduced with permission from [2]. Copyright 1994 Taylor & Francis Ltd.

the scattering centres [2]. In particular, its total resistance cannot be calculated as the sum of the resistances associated with the different scattering centres, because there appears an interference term which is reflected in an exponential behaviour, $R \approx R_0 \exp(L/L_0)$, where R_0 is the resistance quantum, L the system length and L_0 the localization length.

Figure 4, taken directly from [2], illustrates this behaviour, showing for a 1D disordered system how the electron transmission depends on its energy. The sharp peaks in the transmission coefficient are fingerprints of the emergence of strong Anderson localization in these systems and are originated by resonant localized states that are created by disorder [21]. These localized states present an exponential decay away from its centre and, consequently, their resonant width is proportional to $\exp(-l/L_0)$, l being the minimum distance to the system boundaries. This argument shows that the resistance of the 1D disordered system depends strongly on the energy of the incoming electron: electrons resonating with a localized state can have a transmission coefficient close to unity, while for energies away from the resonant states transmission falls to very small values. This fact also explains why the resistance of these 1D disordered systems should show strong fluctuations: moreover, an average of these fluctuations would yield a resistance behaving like $R \approx R_0 \exp(L/L_0)$ (see [2] for a discussion on how this average should be taken).

Our calculations for different SWNTs show a differential conductance with the characteristic behaviour of these 1D systems. In figure 5 we present results for a (5, 5) nanotube with different number of di-vacancies and a different mean distance, d, between defects as calculated using the techniques discussed in section 4; case (a) corresponds to $d = 45.4$ nm and case (b) to $d = 75.5$ nm. Results for 10 di-vacancies are represented in a full line (black), while cases for 20 di-vacancies are represented in a dashed line (red). As mentioned previously, in the discussion of the general properties of disordered 1D systems, we find that the nanotube conductance presents strong fluctuations, with a maximum value close to unity and a minimum that is deeper for an increasing number of di-vacancies. Notice also how the conductance peaks become narrower with the number of di-vacancies and for larger values of d.

Although these results are well known, things are not so well understood if we consider the effect of temperature in the system. It has been thought in this field that the effect of temperature is to introduce inelastic effects in the electron propagation and to destroy the coherence in the electron wavefunctions: if this were the case, one would see experimentally the nanotube resistance to be controlled at room temperature by a diffusive mechanism. This is not, however, the case (as our experimental results reported in section 3 demonstrate), and the reason is that temperature effects do not necessarily destroy the coherent propagation of the electrons. The crucial point to realize is that if $L_\varphi > L$ (see section 2), even at high temperature electrons will propagate from one electrode to the other without suffering inelastic processes; this implies that the main effect of temperature would be to increase the energy window, $k_B T$, the electrons have for their propagation along the nanotube, this window introducing an effective average in the resistance of the system that, as shown below, is going to eliminate the fluctuations in the nanotube resistance without destroying the localization regime. This argument can be expressed more quantitatively in the following way: due to the energy window introduced by the thermal energy, $k_B T$, electrons propagating along the nanotube have a momentum uncertainty given by $\Delta k = k_B T/\hbar v_F$ (v_F is the electron Fermi velocity); this allows us to define the thermal length, L_T, such that $L_T \approx 1/\Delta k \approx \hbar v_F/k_B T$, in such a way that the condition $L_T \cong L_0$ defines the temperature for which the momentum uncertainty introduced by the energy window of the bath destroys the resistance fluctuations (but not the

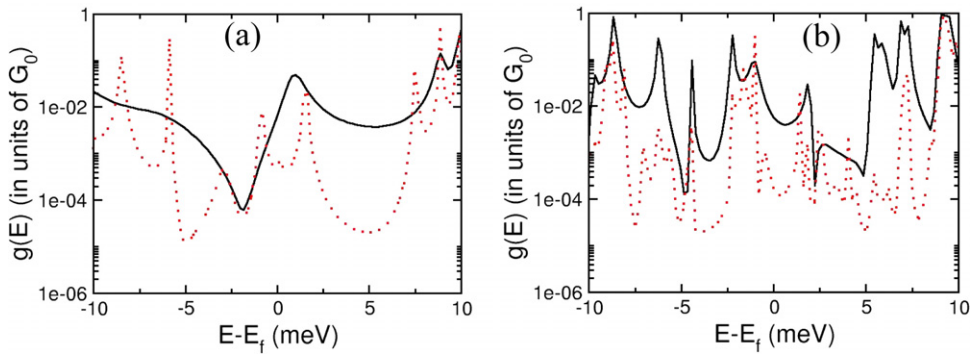

Figure 5. Differential conductance as a function of energy for a (5, 5) nanotube. (a) $d = 45.4$ nm; full line, 10 di-vacancies; dashed line, 20 di-vacancies. (b) As panel (a) but with $d = 75.5$ nm. Notice that the range of energies is between -10 and 10 meV.

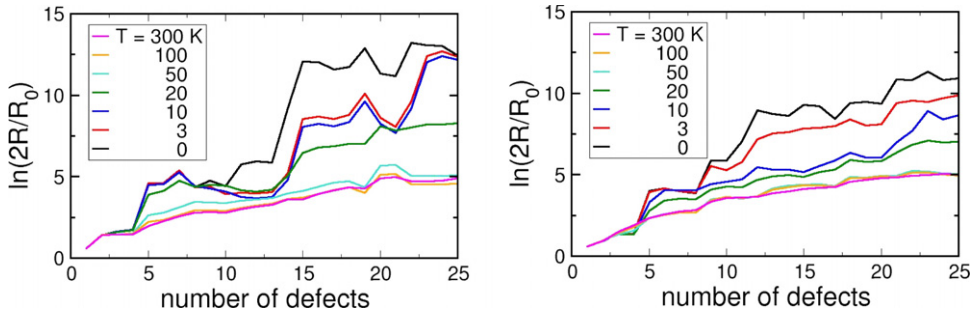

Figure 6. $\ln(2R/R_0)$ as a function of the number of defects, N, and different temperatures for $d = 16.3$ nm (left) and $d = 75.5$ nm (right).

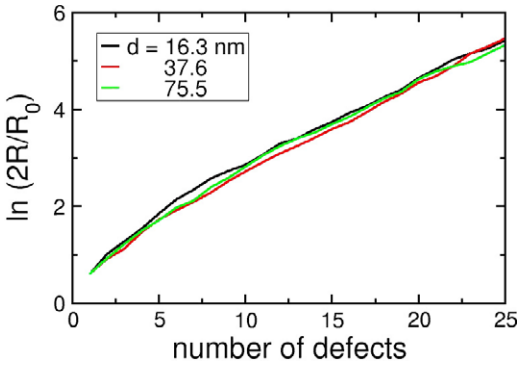

Figure 7. $\langle \ln(2R/R_0) \rangle$ as a function of N at room temperature for different values of d.

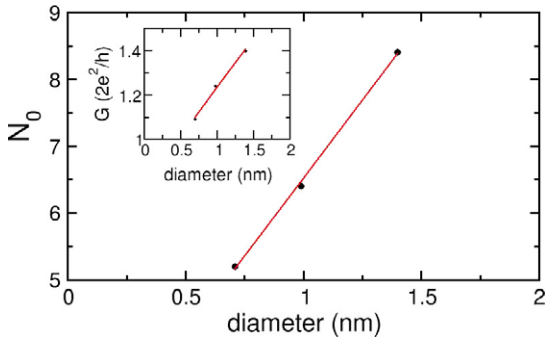

Figure 8. N_0 as a function of the nanotube diameter (the three points shown in the figure correspond to the (5, 5), (7, 7) and (10, 10) nanotubes).The inset also shows G/G_0 for a single di-vacancy in the three SWNTs just mentioned.

localization regime). Notice also that typically, in SWNTs, L_φ is around 1 μm [22], this value suggesting that the pure localization regime could only be observed, even at high T, for nanotubes around or shorter than this length.

In our calculations, temperature is introduced as explained in section 4: this means that we calculate the total intensity (and the resistance) adding all the contributions from all the states included in the thermal energy window. Figure 6 shows $\ln(2R/R_0)$ for a (5, 5) nanotube, as a function of the number of defects for a particular random distribution of di-vacancies and different temperatures, for two different values of d ((a) $d = 16.3$ nm and (b) $d = 75.5$ nm). The crucial point to realize from these two figures is how the resistance fluctuations disappear for increasing values of T: in both cases, a temperature between 20 and 50 K defines the critical value above which the resistance increases exponentially (having no fluctuations) with the number of defects. Another important result we have obtained from our calculations is that the nanotube resistance has a weak dependence on the particular random configuration of di-vacancies and on the mean distance, d, between defects (when the resistance is expressed as a function of the number of defects).

Figure 7 shows our results for the resistance of a (5, 5) nanotube at room temperature (averaged over many different random configurations of defects) and different values of d ($d = 16.3, 37.6$ and 75.5 nm). The reader should compare figures 6 and 7 and realize that the particular random configuration of figures 6(a) and (b) yields a resistance (at room temperature) very close to the averaged values of figure 7. From figure 7 we conclude that the resistance of a (5, 5) SWCNT can be written as

$$R = R_0 \exp(N/N_0), \tag{5}$$

where $N_0 = 5.2$. As $N/N_0 = L/L_0$, we conclude that the localization length, L_0, is given simply by $L_0 = N_0 d$; our results show that, for a (5, 5) nanotube and di-vacancies, the localization length is around five times the mean distance between defects. This is very reasonable result as a di-vacancy is a strong scattering defect creating a large localization of the electronic wavefunctions.

We have also analysed in a similar way the (7, 7) and the (10, 10) SWNTs. Without going into more details, let us only mention that we have found that L_0 appears to be a function of the nanotube diameter. Figure 8 shows N_0 as a function of the nanotube diameter (cases (5, 5), (7, 7) and (10, 10)). Notice the practically linear dependence between N_0 and the nanotube diameter. In the inset of figure 8 we also show the conductance of a single di-vacancy for an (n, n) nanotube: these results show how the localization length is directly related to the di-vacancy conductance, in such a way that di-vacancies having a smaller conductance have a smaller localization length.

6. Conclusions

In conclusion, we have demonstrated, both experimentally and theoretically, the extreme importance of defects (in particular

di-vacancies) in the low bias conducting properties of single-walled carbon nanotubes irradiated with an Ar^+ ion beam. Only 0.1% of di-vacancies produce an increment of several orders of magnitude in the resistance of a 400 nm long SWNT segment. This result is supported by our *ab initio* calculations for the three different nanotubes (5, 5), (7, 7) and (10, 10) analysed in this paper. This behaviour is explained by the strong localization regime created in the 1D system. Our model is a natural and simple way to understand the experiments although, as commented above, it only applies to systems where dissipative interaction is not present. This seems to be the case in SWNTs in the low bias regime. Indeed, assuming a realistic defect density induced by a fixed irradiation dose, the computed localization length L_0 for the (5, 5) and (10, 10) tubes is in very good agreement with experiments not only in absolute value but also showing that there is a strong dependence of the localization length on the tube diameter.

We can summarize the main results that we have obtained for these carbon nanotubes. (i) The transition between the ballistic and the localization regimes occurs for a small number of di-vacancies (about three to five). (ii) For a higher number of defects the system shows localization, the number of effective channels is reduced from two (ballistic) to one [12], and the localization length depends on the tube diameter. (iii) At zero temperature, the nanotube conductance is strongly fluctuating, whereas the effect of finite temperature is to wash out the fluctuations. The exponential scaling behaviour is still preserved at room temperature. Low temperature measurements of irradiated nanotubes will shed light on this fundamental issue. On the other hand, it is not clear whether electron correlation effects (e.g. Luttinger-liquid behaviour) play a role, and this issue has to be resolved by future investigations.

Acknowledgments

This work was partially supported by the Spanish MCyT under contracts MAT2004-01271, MAT2005-01298, MAT2002-01534 and NAN2004-09183-C10, and by Comunidad de Madrid under contract S0505/MAT-0303 and the European Community IST-2001-38052 and NMP4-CT-2004-500198 grants. AR acknowledges support by the European Community Network of Excellence Nanoquanta (NMP4-CT-2004-500198), SANES (NMP4-CT-2006-017310), DNA-NANODEVICES (IST-2006-029192), NANO-ERA-Chemistry projects, the Spanish MEC (FIS2007-65702-C02-01), the Basque Country University (SGIker ARINA) and the Basque Country Government (Grupos Consolidados 2007).

References

[1] Erdos P and Herndon R C 1982 *Adv. Phys.* **31** 65
[2] Pendry J 1994 Symmetry and transport of waves in 1D disordered systems *Adv. Phys.* **43** 461
[3] Lifshitz I M and Kirpichenkov V Y 1979 *J. Exp. Theor. Fiz.* **77** 989
[4] Iijima S 1991 Helical microtubules of graphitic carbon *Nature* **354** 56
[5] Charlier J-C, Blase X and Roche S 2007 Electronic and transport properties of nanotubes *Rev. Mod. Phys.* **79** 677
[6] Loiseau A, Launois P, Petit P, Roche S and Salvetat J-P (ed) 2006 *Understanding Carbon Naotubes* (*Springer Lecture Notes in Physics* vol 677) (Berlin: Springer)
[7] Ebbesen T W (ed) 1997 *Carbon Nanotubes: Preparation and Properties* vol 296 (Tokyo: CRC Press)
[8] Christopher H (ed) 2008 CNT based nanosystems *Advanced Micro and Nanosystems* vol 8 (Weinheim: Wiley-VCH)
[9] Dresselhaus M S, Dresselhaus G and Avouris Ph (ed) 2001 *Carbon Nanotubes: Synthesis, Structure, Properties and Applications* (Berlin: Springer)
[10] Gomez-Navarro C *et al* 2005 *Nat. Mater.* **4** 534
[11] Krasheninnikov A V *et al* 2001 *Phys. Rev.* B **6324** 245405
[12] Biel B *et al* 2006 *Phys. Rev. Lett.* **95** 266801
[13] Datta S 1995 *Electronic Transport in Mesoscopic Systems* (Cambridge: Cambridge University Press)
[14] Sundqvist P *et al* 2007 *Nano Lett.* **7** 2568
[15] Avriller R *et al* 2006 *Phys. Rev.* B **74** 121406
[16] Horcas I *et al* 2007 *Rev. Sci. Instrum.* **78** 013705
[17] de Pablo P J *et al* 2002 *Phys. Rev. Lett.* **88** 36804
[18] Purewal M S *et al* 2007 *Phys. Rev. Lett.* **98** 186808
[19] Demkov A A *et al* 1995 *Phys. Rev.* B **52** 1618
[20] Mingo N *et al* 1996 *Phys. Rev.* B **54** 2225
[21] Anderson P W 1958 *Phys. Rev.* **109** 1492
[22] Javey A *et al* 2003 *Nature* **424** 654
Park J *et al* 2004 *Nano Lett.* **4** 517
Bachtold A *et al* 1999 *Nature* **397** 673
McEuen P L *et al* 1999 *Phys. Rev. Lett.* **83** 5098